Eur. J. Mineral.
2018, **30**, 1127–1132
Published online 6 September 2018

Diatomite as natural precursor for the synthesis of $KAlSiO_4$-*O*1

Daniela NOVEMBRE[1,*], Domingo GIMENO[2] and Brent POE[1]

[1]Dipartimento di Ingegneria e Geologia, Università "D'Annunzio", Via dei Vestini, 31, 66013 Chieti, Italy
*Corresponding author, e-mail: daniela.novembre@unich.it
[2]Departament de Mineralogia, Petrologia i Geoquímica Aplicada, Facultat de Ciències de la Terra, Universitat de Barcelona, Martí i Franquès s/n, 08028 Barcelona, Spain

Abstract: We detail the synthesis and characterization of $KAlSiO_4$-*O*1, a kalsilite polymorph which for years has been considered a material of technological interest. Our experimental protocol requires the preparation of a precursor, obtained by the mixing of potassium hydroxide, aluminium hydroxide and naturally derived amorphous silica (diatomitic rock from Crotone, southern Italy). The precursor was hydrothermally treated at 150 °C and then calcined at 1000 °C. Abundant $KAlSiO_4$-*O*1 phase can be observed after 2 h and its maximum abundance (92%) is observed after 5 h; coexistence with leucite is attested during the time interval 6–100 h.The sample recovered after 5 h was fully characterised by powder X-ray diffraction, He-pycnometry, inductively coupled plasma optical emission spectrometry, infrared spectroscopy and ^{29}Si magic-angle-spinning nuclear magnetic resonance. The amount of amorphous phase in the synthesis powders was estimated with quantitative phase analysis using the combined Rietveld and reference intensity ratio methods.Testing a diatomitic precursor as a source of amorphous silica in the synthesis of $KAlSiO_4$-*O*1 presents both economic and environmental incentives. The high yields and the results of the characterization open the way for the transfer to an industrial production scale.

Key-words: $KAlSiO_4$-*O*1; solid-state synthesis; Rietveld refinement; diatomite; QPA analysis.

1. Introduction

The synthetic phase $KAlSiO_4$-*O*1 represents one of the polymorphs of the mineral kalsilite ($KAlSiO_4$) and for years it has been considered a material of technological interest. For example, high-thermal-expansion ceramics have been prepared from $KAlSiO_4$-*O*1 for bonding on copper or silver (Ota *et al.,* 1996). The material is of considerable importance in the context of high-temperature technologies, as it has been used in blast-furnace linings (Rigby & Richardson, 1947), magnetohydrodynamic generators (Cook *et al.*, 1977) and hazardous-waste incinerator clinkers (Li *et al.*, 2003). It also occurs as a rock-forming mineral in pyrometamorphic rocks of the Hatrurim Complex, Negev Desert, Israel (Krüger *et al.*, 2016).

$KAlSiO_4$-*O*1 was first synthesized by Cook *et al.* (1977) and its structure refined with orthorhombic symmetry in the space group $P2_12_12$. Later, a refinement by Gregorkiewitz *et al.* (2008) determined the space group as $P12_11$. Kremenović *et al.* (2013) resolved the structure of single crystals of $KAlSiO_4$-*O*1 in the monoclinic system ($P2_1$). Cook *et al.* (1977) investigated the transformations of $KAlSiO_4$-*O*1 into the polymorph $KAlSiO_4$-O2 at temperatures higher than 1450 °C.

$KAlSiO_4$-*O*1 has been synthesized in the past in a temperature range between 950 °C and 1300 °C by the solid-state method (Dimitrijevic & Dondur, 1995; Ota *et al.*, 1996; Cook *et al.*, 1977; Gregorkiewitz *et al.*, 2008) or by the flux technique (Kremenović *et al.*, 2013). In all of these previous studies, the authors chose the use of commercial reagents as starting materials for the synthesis procedure, such as SiO_2 or amorphous silica gel, Al_2O_3, K_2CO_3, KVO_3 (Cook *et al.*, 1977; Gregorkiewitz *et al.*, 2008; Kremenović *et al.*, 2013), zeolite LTA and KCl solutions (Dimitrijevic & Dondur, 1995).

The first aim of this work is to develop a new experimental protocol for the synthesis of $KAlSiO_4$-*O*1, which follows a two-step process: first, the preparation of a hydrothermally derived precursor and then the calcination of the precursor at high temperature. The precursor is prepared starting from a silica source, potassium hydroxide and aluminium hydroxide. A novel starting material used as the silica source is tested, *i.e.* a naturally derived amorphous silica (a diatomitic rock from Crotone, southern Italy). This natural, inexpensive and abundant geologic resource has recently been used in other successful synthesis processes, particularly for the preparation of zeolitic minerals (Boukadir *et al.*, 2002; Sanhueza *et al.,* 2003, 2004; Novembre *et al.*, 2004, 2014). A natural, cost-effective starting material makes this route especially attractive when expanded to an industrial scale as long as the material properties of the $KAlSiO_4$-*O*1 product remain satisfactory.

0935-1221/18/0030-2782 $ 2.70
https://doi.org/10.1127/ejm/2018/0030-2782

2. Methods

Products of syntheses were analysed by powder X-ray diffraction (XRPD) using a Siemens D5000 operating with a Bragg-Brentano geometry; Cu $K\alpha$ = 1.518 Å, 40 kV, 40 mA, 2–45° scanning interval, step size 0.020° 2θ. Identification of phases and relative peak assignments were performed with reference to the JCPDS codes 00-033-0989 for $KAlSiO_4$-*O*1 and 00-038-1423 for leucite.

The amounts of both the crystalline and amorphous phases in the synthesis powders were estimated using Quantitative Phase Analysis (QPA) applying the combined Rietveld and Reference Intensity Ratio (RIR) methods; corundum NIST 676a was added to each sample, amounting to 10% by weight (according to the strategy proposed by Novembre *et al.*, 2017), and the powder mixtures were homogenized by hand-grinding in an agate mortar. Data for the QPA refinement were collected in the range 5–80° 2θ with steps of 0.02° 2θ and 10 s $step^{-1}$, a divergence slit of 0.5° and a receiving slit of 0.1 mm.

Data were processed with the GSAS software (Larson & Von Dreele, 1997) and the graphical interface EXPGUI (Toby, 2001). The unit-cell parameters were determined, starting with the structural models proposed by Kremenović *et al.* (2013) for $KAlSiO_4$-*O*1 and Dove *et al.* (1993) for leucite. The following parameters were refined: background parameters, zero shift, cell parameters and peak profiles.

Chemical analysis on synthesized powders was achieved by inductively coupled plasma optical emission spectroscopy (Perkin Elmer AS-90 Plus) after alkaline fusion of the sample in a Pt crucible (lithium meta-tetraborate pearls, at 3/2 ratio) and subsequent acid solubilisation (as explained in Novembre *et al.*, 2005, 2011). Each sample was fused in duplicate and the crucibles were cleaned each time by alkaline fusion plus acid bath. Standard solutions were also prepared for each analysis. The standards were prepared by traditional wet methods from a certified commercial traceable list. International rock standards (provided by the Geological Survey of Japan, GSJ) were also analysed in order to gauge analytical error.

Scanning electron microscope (SEM) analyses were carried out with a JEOL JSM-840 with operating conditions of 15 kV and window conditions ranging from 18 to 22 mm, following the procedure explained in Ruggieri *et al.* (2011). Also, a double coating (graphite plus vaporised Au) of the sample was chosen (see Novembre *et al.*, 2004).

Densities of kalsilite and $KAlSiO_4$-*O*1 were measured by He-picnometry using an AccuPyc 1330 pycnometer.

The Infrared (IR) spectroscopic studies of the synthesized products were conducted with a FTLA2000 spectrometer, equipped with KBr beamsplitter and DTGS detector; the source of IR radiation was a SiC (Globar) filament. Samples were prepared according to the method of Robert *et al.* (1989a) using powder pressed pellets (sample-to-KBr ratio of 1/100 at a load force of 15 t cm^{-2}); spectra were processed with the program GRAMS-Al.

The ^{29}Si magic-angle-spinning nuclear magnetic resonance (^{29}Si MAS NMR) study was performed with a Bruker Avance-Spectrospin 300 MHz (4 kHz rotational frequency at the magic angle, variable number of scans from: 100, 200 to 400, pulse length (90°) $p1$ = 8 µs and scanning time ($t1$ = 5 s); the spectra were processed with the program Bruker WINNMR. The chemical shifts were referenced to trimethylsilyl propionic (2,2,3,3)-d_4 acid, sodium salt (TSP) for ^{29}Si.

2.1. Siliceous raw material: "Tripoli rock"

The starting material was a diatomite, *i.e.* a tripolaceous siliceous rock (Tripoli rock) cropping out in the Crotone Basin in southern Italy. Characterization of this material (see Novembre *et al.*, 2004, 2014) reveals a mineralogical assemblage mainly made of an amorphous siliceous fraction (diatoms and sponges), quartz, montmorillonite, chlorite, kaolinite, K-micas and small amounts of carbonates. There is evidence of vertical and lateral variability in the incidence of the above phases all over the deposit.

2.2. Preparation of reagents from natural rocks

2.2.1. Siliceous solution

According to the method proposed by Novembre *et al.* (2004, 2014), 5.19 g of the ground and powdered Tripoli material were treated with HNO_3, in order to dissolve the carbonate fraction as well as other impurities such as nitrate compounds. The diatomitic sample (5 g after the HNO_3 treatment) was added to 40 mL of KOH (8.5%) and to 10 mL of deionized water.

This solution was accurately mixed with a magnetic stirrer for 2 h and then put in a teflon reactor/bomb and heated in an oven at 80 °C for 24 h. After filtration, the remnant solid and insoluble fraction, which consisted of clay minerals and quartz, was separated from the silicate solution. After the insoluble solid fraction was separated, the K-solution was filtered. The resulting molar composition of the solution was 0.060 K_2O–0.026 SiO_2–0.625 H_2O with traces as follows: 2.01 ppm Mg, 2.11 ppm Ca and Al, Ti and Mn lower than 0.1 ppm.

After the chemical treatments, the Tripoli rock was determined to be composed of: 32 wt% amorphous silica (diatoms and sponges), 63.27 wt% of clay minerals and quartz, and 3.83 wt% carbonates.

2.2.2. Aluminous solution

0.45 g of $Al(OH)_3$ (65%) were mixed to 40 mL of KOH (8.5%) and 10 mL of deionized water. The obtained aluminous solution with a composition of 0.060 K_2O–0.0076 Al_2O_3–0.625 H_2O (Mn, Ti and Mg < 0.01 ppm; Fe < 0.4 ppm; K, Ca and Si < 0.2 ppm) was then heated at 100 °C for one hour.

3. Synthesis of $KAlSiO_4$-*O*1

Synthesis was carried out by mixing 5 mL of the siliceous solution to 10 mL of the aluminous solution. From the

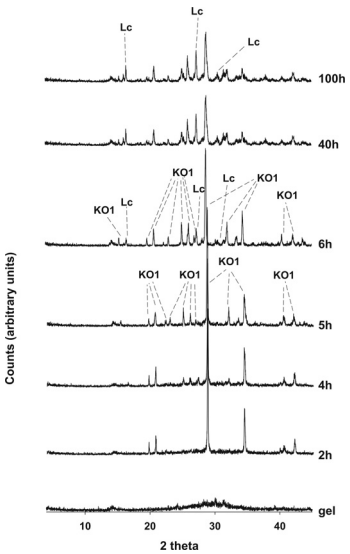

Fig. 1. X-ray diffractometric sequence of the synthesis run.

two given starting solutions the synthesis solution has a SiO_2/Al_2O_3 ratio greater than the stoichiometry of kalsilite. In the preparation of the synthesis mixture, in fact, we accounted for the different solubilities of SiO_2 compared to Al_2O_3 in an alkaline solution; for example, in order to obtain a kalsilite characterized by an SiO_2/Al_2O_3 ratio equal to 2, one must start from a mixture characterized by an excess of silica (SiO_2/Al_2O_3 up to 4), and also the aqueous medium has to contain additional potassium hydroxide with respect to the stoichiometry of kalsilite, as previously explained by Barrer *et al.* (1959) for the hydrothermal synthesis of silicates.

The reactants were rigorously mixed for two hours with a magnetic stirrer. The mixture was heated inside autoclaves at 150 °C and ambient pressure for a duration of 1 h. The hydrothermally derived gel precursor was sampled from the reactors, filtered from the solution, thoroughly washed with distilled water in order to remove excess KOH, and dried in an oven at 40 °C for 24 h. Characterization by XRPD analysis (Fig. 1) showed the resulting material to be amorphous. The gel precursor was then calcined at 1000 °C and sampled at scheduled interval times.

4. Result and discussion

4.1. Mineralogical, crystallographic and chemical characterization of synthetic products

The crystallization of the synthetic KAlSiO$_4$-*O*1 phase is evident within the time interval 2–5 h. After this time, the presence of KAlSiO$_4$-*O*1 is associated to that of leucite in the time interval 6–100 h, *i.e.*, the experimental run ends with a final overlapping of the two phases.

A possible mechanism is that KAlSiO$_4$-*O*1 would crystallize at first, then react with excess silica finally forming leucite. Actually, replacement of KAlSiO$_4$-*O*1 by leucite with time is consistent with the finding by Zhang *et al.* (2007). These authors, in fact, have found kalsilite as the common metastable phase during the leucite crystallization process when calcinating at temperatures ranging from 750° to 900 °C.

The observed and calculated profiles and difference plots for KAlSiO$_4$-*O*1, leucite and corundum NIST 676a are reported for the samples at 2, 4, 5, 6, 40 and 100 h as Figs. S1 and S2 in the Supplementary Material linked to this article and freely available at https://pubs.geoscienceworld.org/eurjmin. The cell parameters of KAlSiO$_4$-*O*1, refined with monoclinic symmetry, space group $P2_1$, and of leucite, refined with tetragonal symmetry, space group $I4_1/a$, are reported in Table 1 together with the results of the QPA analysis. Cell parameters for both KAlSiO$_4$-*O*1 and leucite remain constant within error as a function of the experimental run time.

Figure 2 illustrates the volume or weight fractional changes in the participating phases as a function of time. The most notable changes occur over the first 2 h of the synthesis as nearly 75% of the amorphous phase is transformed directly into KAlSiO$_4$-*O*1. From 2 to 5 h, this transformation appears to slow down during which the maximum KAlSiO$_4$-*O*1 fraction of 92.55% is reached before any leucite is detected. After 5 h, the KAlSiO$_4$-*O*1 phase is continually replaced by leucite, even though about 6–7% of the sample remains amorphous. At 100 h, the sample is dominated by the presence of leucite (61.62%).

Further characterizations have been performed on the sample obtained at 5 h, it being constituted mainly by KAlSiO$_4$-*O*1. Figure 3 reports an SEM image of typical KAlSiO$_4$-*O*1 crystals from this sample, with an average maximum length of crystals observed to be around 4 μm. In Table 2 we report the chemical analysis and a resulting stoichiometry of $(K_{7.15})(Al_{7.76}Si_{8.39})O_{32}$. The Si/Al ratio of 1.08 is in good agreement with the results of Stebbins *et al.* (1986), who obtained a ratio of 1.06 for a kalsilite synthesized starting from oxides. The same can also be said for the small excess of Si compared to K that is highlighted in the formula both in our case and in that of the aforementioned authors, as lesser potassium is required to charge-balance Al tetrahedral sites for ratios of Si/Al > 1. The density of KAlSiO$_4$-*O*1 from this sample was determined to be 2.653(5) g cm^{-3}, which is comparable to those obtained by Gregorkiewitz *et al.* (2008) of 2.57 g cm^{-3} and Kremenović *et al.* (2013) of 2.597 g cm^{-3}.

4.2. Infrared analysis and ^{29}Si magic angle spinning nuclear magnetic resonance

The infrared spectrum of KAlSiO$_4$-*O*1 is shown in Fig. 4. Frequencies of absorption bands found here are compiled in Table 3 together with known data for KAlSiO$_4$-*O*1 (Dimitrijevic & Dondur, 1995). Eight partially resolved bands can be identified in the high-frequency portion of the spectrum due to Si–O stretching vibrations (1106, 1072, 1033, 988, 973, 958, 942 and 930 cm^{-1}). Two additional bands with lower shifts are located at 692 and 664 cm^{-1}, which are similar in frequency to those observed

Table 1. Experimental conditions and crystallographic data for $KAlSiO_4$-*O*1 and leucite plus corundum NIST 676a: samples at 2, 4, 5, 6, 40 and 100 h.

Sample + 10 wt% corundum NIST 676a	2 h	4 h	5 h	6 h	40 h	100 h
R_{wp}	0.19	0.21	0.18	0.22	0.17	0.21
R_p	0.2	0.13	0.14	0.16	0.12	0.15
CHI^2	2.83	2.43	2.52	2.66	1.5	2.39
Space group $KAlSiO_4$-*O*1	$P2_1$	$P2_1$	$P2_1$	$P2_1$	$P2_1$	$P2_1$
a (Å)	15.6412(51)	15.6433(39)	15.6418(45)	15.6503(57)	15.6512(37)	15.5983(49)
b (Å)	9.0315(5)	9.0402(6)	9.0319(5)	9.0435(5)	9.0323(7)	9.0344(4)
c (Å)	8.5918(7)	8.5865(6)	8.5844(9)	8.5712(8)	8.5911(8)	8.5833(9)
β (°)	89.9703(23)	89.9872(11)	89.9821(25)	89.9799(14)	89.9092(22)	89.9633(12)
Space group leucite				*I*41/*a*	*I*41/*a*	*I*41/*a*
a (Å)				13.0763(34)	13.0812(37)	13.0822(48)
b (Å)				13.0773(41)	13.0824(43)	13.0811(49)
c (Å)				13.7466(39)	13.7514(31)	13.7469(53)
% Amorphous	25.65(11)	17.2(8)	7.45(12)	7.2(8)	6.53(19)	6.3(16)
% Leucite	0	0	0	20.36(17)	50.85(19)	61.62(18)
% $KAlSiO_4$-*O*1	74.35(14)	82.8(8)	92.55(19)	72.44(17)	42.62(18)	32.08(18)

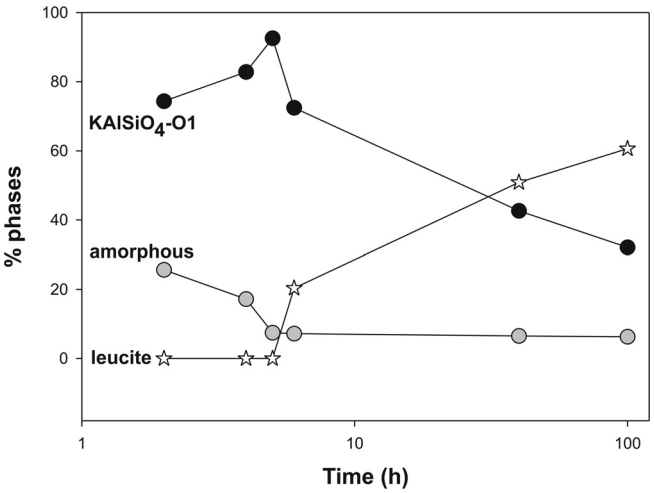

Fig. 2. Weight fractional changes of phases as a function of time.

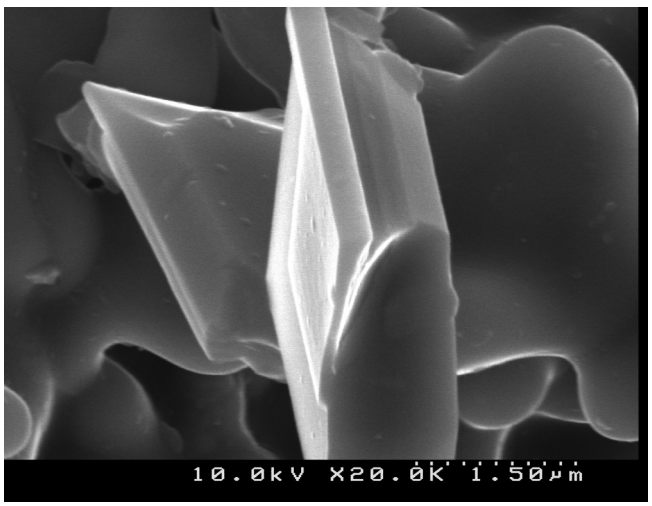

Fig. 3. SEM image of a $KAlSiO_4$-*O*1 crystal obtained at 5 h of synthesis run.

by Dimitrijevic & Dondur (1995), who interpreted them as being due to symmetric Si–O stretching modes. It is more likely that these lower-frequency vibrations are due to Al–O stretching motions as its bond strength is weaker than that of the tetrahedral Si–O bond.

The ^{29}Si NMR spectrum is characterized by a band located at −85.58 ppm (Fig. 5), in good agreement with Stebbins *et al.* (1986) for a $Q^4(4Al)$ site. Due to the low signal-to-noise ratio of the spectrum as the sample was not isotopically enriched, we are unable to detect other possible Si species, whereas Stebbins *et al.* (1986) observed a secondary resonance feature at −93.9 ppm (Table 4).

5. Conclusions

This work describes the synthesis of $KAlSiO_4$-*O*1 using a natural, inexpensive and abundant geologic resource combined with a simple, but novel chemical process. A precursor, prepared through a series of chemical treatments performed on a sample of diatomitic rock coming from Crotone (Italy), was hydrothermally treated at temperature of 150 °C and successively calcined at 1000 °C. The presence of $KAlSiO_4$-*O*1 as isolated phase is attested in the time interval 2–5 h. In particular the maximum abundance of $KAlSiO_4$-*O*1 is observed at 5 h, after which the phase is steadily replaced by leucite. The QPA analyses indicate a product at 5 h contituted by 92.55% $KAlSiO_4$-*O*1 and 7.45% amorphous component. The chemical-physical and spectroscopic characterization of the sample at 5 h underscore the efficiency of the experimental procedure proposed here. The results from infrared and NMR spectroscopic analyses are comparable with those reported in the literature for $KAlSiO_4$-*O*1.

Quantitative data suggest that transfer to an industrial production scale would be possible. In addition, the use of amorphous silica obtained by a georesource, in place of commercial amorphous silica, confers uniqueness and considerable low cost to the protocol, while enhancing a natural material through its use in a synthesis process.

Table 2. Chemical characterization (wt%) of KAlSiO$_4$-*O*1 (sample at 5 h). Values for the MgO, MnO, TiO_2 and P_2O_5 oxides are under the detection limits.

T (°C)	K_2O	SiO_2	Al_2O_3	Time	PXRD spectrum
1000	27.21	40.73	31.95	5 h	KAlSiO$_4$-*O*1
1446	26.00	40.60	32.10	4 d	KAlSiO$_4$-*O*1*

*Stebbins *et al*. (1986).

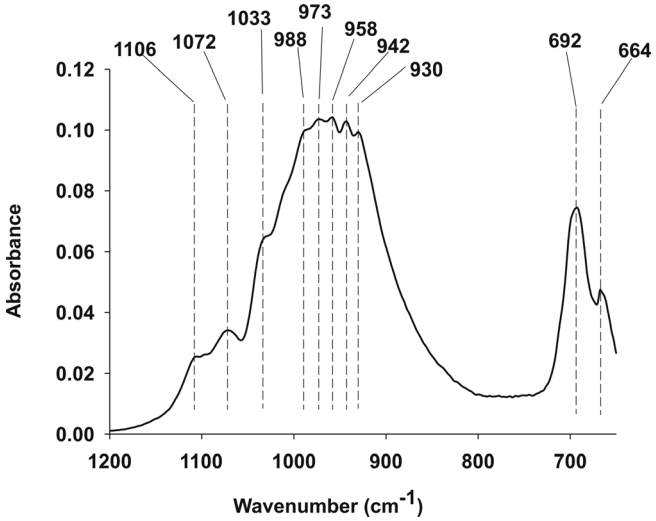

Fig. 4 Infrared spectrum of sample at 5 h.

Table 3. Asymmetric stretch of inner bonds and symmetric stretch of external bonds of tetrahedra for sample at 5 h of the experimental run.

Sample	as T-O-T	s T-O-T
5 h	1106-1072-1033-988-973-958-942-930	692-664
KAlSiO$_4$-*O*1*	1100-1070-1040-990-940-880	700-665

*Dimitrijevic & Dondur (1995).

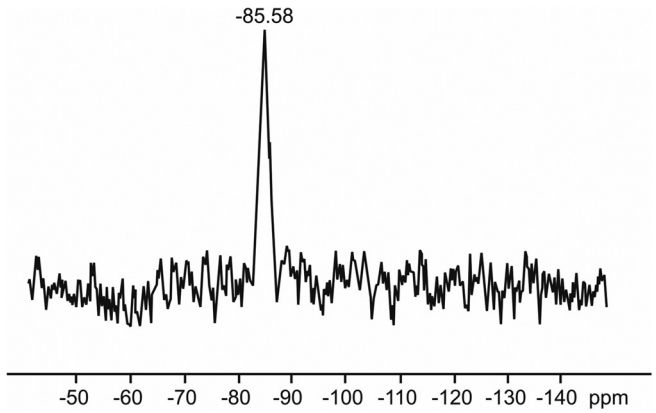

Fig. 5 ^{29}Si Mas-NMR spectrum of sample at 5 h.

Table 4. ^{29}Si Chemical Shift (ppm) for sample at 5 h.

Sample	^{29}Si Chemical shift (ppm)
5 h	−85.58, (−89.2)
KAlSiO$_4$-*O*1*	−84.9, −88.5, (−93.9)
KAlSiO$_4$-*O*1**	−85.6, −88.8, (−92.0, −97.0)

*Stebbins *et al.* (1986), KAlSiO$_4$-*O*1 grown by high-temperature sintering of oxides.
**Stebbins *et al.* (1986), KAlSiO$_4$-*O*1 obtained after thermal treatment of kalsilite.

Acknowledgements: The authors greatly acknowledge the technical staff at Centres Cientifics i Tecnologics of Barcelona University for their help during the development of the work.

References

Barrer, R.M., Baynham, J.W., Bultitude, F.W., Meier, W.M. (1959): Hydrothermal chemistry of the silicates. Part VIII. Low temperature crystal growth of aluminosilicates, and of some Gallium and Germanium analogues. *J. Chem. Soc.*, **36**, 195–208.

Boukadir, D., Bettahar, N., Derriche, Z. (2002): Etude de la synthèse des zéolites 4A et HS à partir de produits naturels. *Ann. Chim. – Sci. Mat.*, **27**, 1–13.

Cook, L.P., Roth, R.S., Parker, H.S., Negas, T. (1977): The system K_2O-Al_2O_3-SiO_2. Part 1. Phases on the KAlSiO$_4$-$KAlO_2$ join. *Am. Mineral.*, **62**, 1180–1190.

Dimitrijevic, R. & Dondur, V. (1995): Synthesis and characterization of KAlSiO$_4$ polymorphs on the SiO_2-$KAlO_2$ join. II. The end-member of ANA-type zeolite framework. *J. Solid State Chem.*, **115**, 214–224.

Dove, M.T., Cool, T., Palmer, D.C., Putnis, A., Salje, E.K.H., Winkler, B. (1993): On the role of Al-Si ordering in the cubic-tetragonal phase transition of leucite. *Am. Mineral.*, **78**, 486–492.

Gregorkiewitz, M., Li, Y., White, T.J., Withers, R.L., Sobrados, I. (2008): The structure of "orthorhombic" KAlSiO4–*O*1: evidence for Al-Si order from MAS NMR data combined with Rietveld refinement and electron microscopy. *Can. Mineral.*, **46**, 1511–1526.

Kremenović, A., Lazic, B., Krüger, H., Tribus, M., Vulić, P. (2013): Monoclinic structure and nonstoichiometry of "KAlSiO4–*O*1". *Acta Crystallogr.*, **C69**, 334–336.

Krüger, B., Krüger, H., Tropper, P., M. Tribus, , Joachim, B. (2016): First natural occurence of "KAlSiO4–*O*1". Abstracts 2nd European Mineralogical Conference, , Rimini, Italy, , 11–15 September, http://emc2016.socminpet.it/documents/Book-of-Abstracts_emc2016_small.pdf, 413 p.

Larson, A.C., & Von Dreele, R.B. (1997): GSAS: General Structure Analysis System *Document Laur 86-748*, Los Alamos National Laboratory.

Li, Ying., Laursen, K., White, T.J., Gregorkievitz, M. (2003): The crystal chemistry and microstructure of fluidised bed incinerator clinker tridymite. *Journal Material and Engineering*, **14**, 119–125.

Novembre, D., Di Sabatino, B., Gimeno, D., Garcia Valles, M., Martinez-Manent, S. (2004): Synthesis of Na-X zeolites from tripolaceous deposits (Crotone, Italy) and volcanic zeolitized rocks (Vico Volcano, Italy). *Microporous Mesoporous Mater.*, **75**, 1–11.

Novembre, D., Di Sabatino, B., Gimeno, D. (2005): Synthesis of Na-A zeolite from 10Å halloysite and a new crystallization kinetic model for the transformation of Na-A into HS zeolite. *Clays Clay Minerals*, **53**, 28–36.

Novembre, D., Di Sabatino, B., Gimeno, D., Pace, C. (2011): Synthesis and characterization of Na-X, Na-A, Hydroxisodalite and Na-P zeolites from metakaolinite. *Clay Minerals*, **46**, 336–354.

Novembre, D., Pace, C., Gimeno, D. (2014): Syntheses and characterization of zeolites K-F and W type using a diatomite precursor. *Mineral. Mag.*, **78**, 1209–1225.

—,—,— (2017): Synthesis and characterization of wollastonite-2*M* by using a diatomite precursor. *Mineral. Mag.*, **82**, 95–110.

Ota, T., Takebayashi, T., Takahashi, M., Hikichi, Y. (1996): High thermal expansion $KAlSiO_4$ ceramic. *J. Mater. Sci.*, **31**, 1431–1433.

Rigby, G.R. & Richardson, H.M. (1947): The occurrence of artificial kalsilite and allied potassium aluminum silicates in blast furnace linings. *Mineral. Mag.*, **28**, 75–88.

Robert, J.-L., Della Ventura, G., Thauvin, J.L. (1989): The infrared OH-stretching region of synthetic richterites in the system Na_2O–K_2O-CaO-MgO-SiO_2–H_2O-HF. *Eur. J. Mineral.*, **1**, 203–211.

Ruggieri, F., Fernandez–Turiel, J.L., Saavedra, J., Polanco, E., Naranjo, J.A. (2011): Environmental geochemistry of recent volcanic ashes from Southern Andes. *Environmental Chemistry*, **8**, 236–247.

Sanhueza, V., & Kelm, U., Cid, R. (2003): Synthesis of mordenite from diatomite: a case of zeolite syntesis from natural material. *J. Chem. Technol. Biotechnol.*, **78**, 485–488.

Sanhueza, V., Kelm, U., Cid, R., Lòpez-Escobar, L. (2004): Synthesis of MSM-5 from diatomite: a case of zeolite synthesis from a natural material. *J. Chem. Technol. Biotechnol.*, **79**, 686–0690.

Stebbins, J.F., Murdoch, J.B., Carmichael, I.S.E., Pines, A. (1986): Defects and short-range order in nepheline group minerals: a Silicon-29 Nuclear Magnetic Resonance study. *Phys. Chem. Miner.*, **13**, 371–381.

Toby, B.H. (2001): EXPGUI, a Graphical User Interface for GSAS. *J. Appl. Crystallogr.*, **34**, 210–213.

Zhang, Y., Lv, M., Chen, D., Wu, J. (2007): Leucite crystallization kinetics with kalsilite as a transition phase. *Mater. Lett.*, **61**, 2978–2981.

Received 14 November 2017
Modified version received 12 December 2017
Accepted 27 April 2018